



Pergamon

# Design and Synthesis of Poly(ADP-Ribose) Polymerase-1 (PARP-1) Inhibitors. Part 4: Biological Evaluation of Imidazobenzodiazepines as Potent PARP-1 Inhibitors for Treatment of Ischemic Injuries

Dana Ferraris,\* Rica Pargas Ficco, David Dain, Mark Ginski, Susan Lautar, Kathy Lee-Wisdom, Shi Liang, Qian Lin, May X.-C. Lu, Lisa Morgan, Bert Thomas, Lawrence R. Williams, Jie Zhang, Yinong Zhou and Vincent J. Kalish

*Guilford Pharmaceuticals Inc., 6611 Tributary Street, Baltimore, MD 21224, USA*

Received 14 May 2003; accepted 16 May 2003

**Abstract**—A class of poly(ADP-ribose) polymerase (PARP-1) inhibitors, the imidazobenzodiazepines, are presented in this text. Several derivatives were designed and synthesized with ionizable groups (i.e., tertiary amines) in order to promote the desired pharmaceutical characteristics for administration in ischemic injury. Within this series, several compounds have excellent in vitro potency and our computational models accurately justify the structure–activity relationships (SARs) and highlight essential hydrogen bonding residues and hydrophobic pockets within the catalytic domain of PARP-1. Administration of these compounds (**5q**, **17a** and **17e**) in the mouse model of streptozotocin-induced diabetes results in maintenance of glucose levels. Furthermore, one such inhibitor (**5g**,  $IC_{50} = 26$  nM) demonstrated significant reduction of infarct volume in the rat model of permanent focal cerebral ischemia.

© 2003 Elsevier Ltd. All rights reserved.

## Introduction

Poly(ADP-ribose) polymerase-1 (PARP-1, EC 2.4.2.30) also known as poly(ADP-ribose) synthetase is an abundant nuclear enzyme with an important role in the cellular life cycle.<sup>1–3</sup> The PARP-1 enzyme has three important structural domains: the DNA binding domain containing two zinc fingers, the automodification domain and the catalytic domain.<sup>4,5</sup> The catalytic domain is responsible for converting nicotinamide adenine dinucleotide (NAD<sup>+</sup>) into nicotinamide and an ADP-ribose unit that is attached to either PARP-1 itself or other proteins.<sup>6</sup> During normal cell division, PARP-1 is involved with repairing damaged DNA and for this reason inhibitors of this enzyme have been utilized as an adjunct for cancer chemotherapy treatment.<sup>7</sup> When overactivated, however, PARP-1 can cause extensive polymerization of ADP-ribose, leading to the

depletion of NAD<sup>+</sup> and, subsequently, a decrease in the level of intracellular ATP. This depletion of ATP results in cell death through a necrotic pathway.<sup>8,9</sup> Earlier studies done with PARP-1 ‘knockout’ mice demonstrated that a lack of PARP-1 offers protection in animal models of stroke<sup>10</sup> and heart ischemia.<sup>11,12</sup> More recently, PARP-1 has also been implicated in the destruction of  $\beta$ -islet cells in diabetic mice.<sup>13–15</sup> These data indicate that PARP-1 may be a clinically relevant target for ischemia/reperfusion injuries, and the progression of type 1 diabetes mellitus, two areas of medicine with unmet therapeutic needs.

Most of the published inhibitors of PARP-1 have a common structural motif, namely the benzamido moiety (outlined in bold, Fig. 1) as shown in substituted benzamides **1**,<sup>16</sup> isoquinolones **2**,<sup>17</sup> and 5[*H*]phenanthridin-6-ones **3**.<sup>18,19</sup> Structural studies indicate that this amide forms three important hydrogen bonds with two amino acid residues in the catalytic domain of PARP-1, namely Ser904 and Gly863. Removal or alteration of this amide moiety and disruption of these hydrogen

\*Corresponding author. Tel.: +1-410-631-8126; fax: +1-410-631-6797; e-mail: ferrarisd@guilfordpharm.com

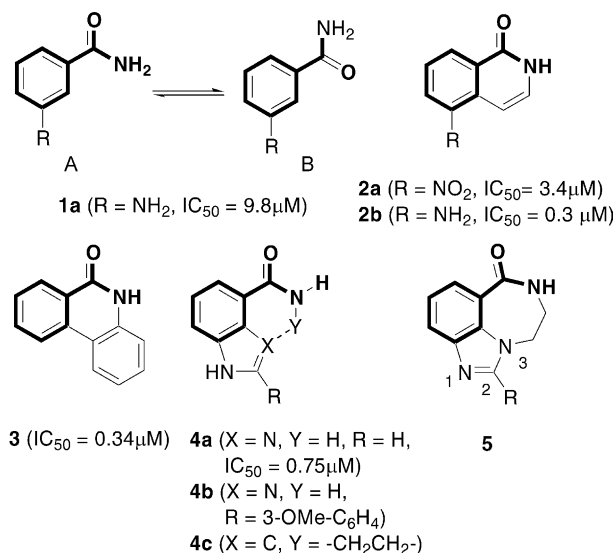


**Figure 1.** Classes of PARP-1 inhibitors.

bonds results in compounds with negligible activity in almost every instance.<sup>20</sup> In addition, the conformation of this amide is important to potency. That is, there are two equally populated conformations for this amide in this ‘first-generation’ benzamide series (**1**, A and B, Fig. 1). The preferred conformation of this amide in the active site, however, is illustrated by conformation A.<sup>21,22</sup> Hence, constraining this amide within an adjacent ring (mimicking conformation A) led to a ‘second generation’ of compounds that were over an order of magnitude more potent than the ‘first-generation’ benzamides as shown in the isoquinolone and 5[*H*]-phenanthridin-6-one series.

The benzimidazoles **4a–b** were concurrently designed with the idea of elegantly forcing this amide into the desired conformation through an intramolecular hydrogen bond (**4a** and **4b**, X = N, Y = H, Fig. 1). Using various methods to synthesize benzimidazoles, a wide variety of 2-substituted analogues were made which demonstrated good PARP-1 inhibition.<sup>20</sup> In addition, crystallographic studies confirmed the importance of conformation A (Fig. 1), the size of the nicotinamide binding pocket and the tolerance for large substituents at the 2-position. Formation of a third ring (seven membered) in place of this intramolecular hydrogen bond has also been done recently, leading to a new series of tricyclic PARP-1 inhibitors (**4c**, X = C, Y = -CH<sub>2</sub>CH<sub>2</sub>-Fig. 1) with similar SAR to the benzimidazoles and in vitro potency in models of cellular growth inhibition.<sup>23,24</sup>

We report herein the synthesis and in vitro activity of imidazobenzodiazepines **5** as a related series of tricyclic PARP-1 inhibitors (Fig. 1). This class of compounds was initially designed to restrict the conformation of the amide pharmacophore within a seven-membered ring analogous to the recent tricyclic indoles.<sup>24</sup> Understanding the relative tolerance that PARP-1 has for bulky substituents at the 2-position of benzimidazoles,

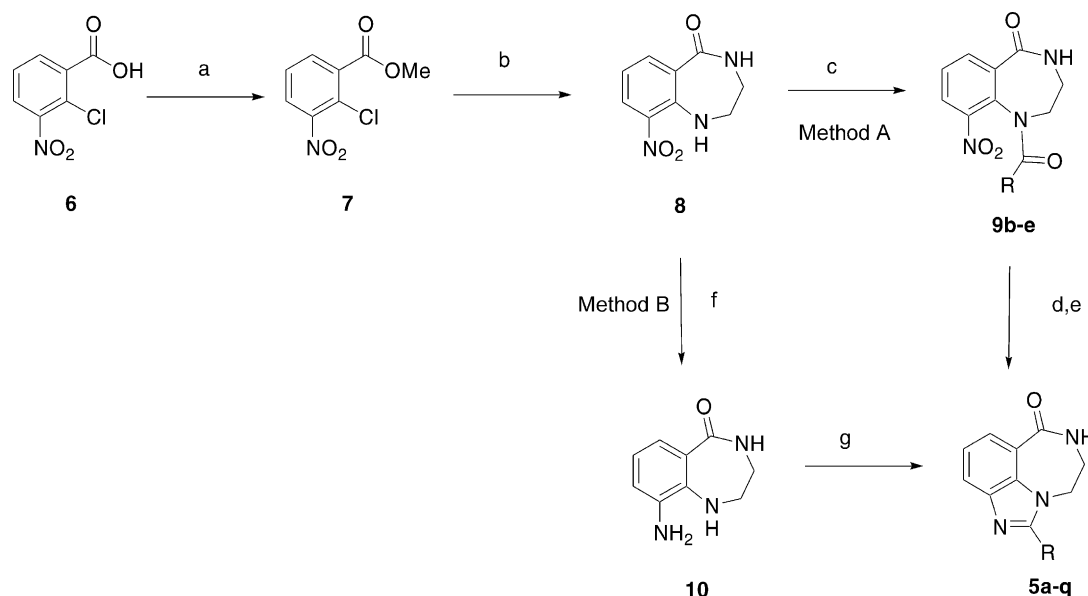
we decided to derivatize at this position in order to improve the pharmaceutical characteristics of our compounds without the loss of in vitro potency. In this paper, in vitro potencies and permeability analysis were gathered for representative members of this series. Most importantly, selected imidazobenzodiazepines were found to be efficacious in animal models of diabetes and stroke and the results from these studies will be reported herein.

## Chemistry

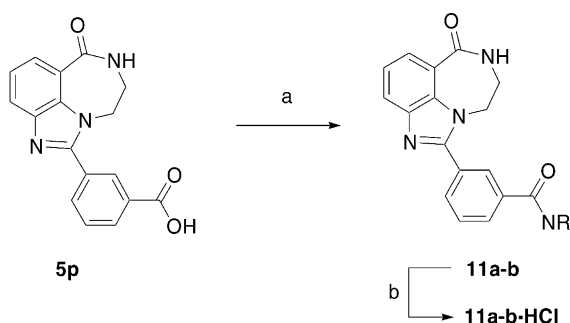
The initial synthesis of imidazobenzodiazepines is outlined in Scheme 1 (Method A). The commercially available benzoic acid **6** was esterified to methyl ester **7** via the acid chloride in 95% yield.<sup>25</sup> The formation of the seven-membered diazepine ring was accomplished by refluxing with ethylene diamine in *n*-butanol to afford nitro diazepine **8** in 84% yield. Derivatization of compound **8** was accomplished by acylation with the requisite acid chlorides leading to amides **9b–e**. Although nitro amides **9b–e** were reduced quantitatively, the subsequent cyclization step required refluxing in toluene over extended periods of time affording compounds **5b–e** in low yield.

This prompted us to explore an alternative synthetic route from **8** to **5** as outlined in Scheme 1 (Method B). The nitro diazepine **8** was reduced in the presence of Raney nickel and hydrazine to yield amine **10** in 94% yield. Various aldehydes reacted with this diamine in the presence of palladium on carbon to form the benzimidazole ring in moderate to good yield (30–82%). All of the final products were easily recrystallizable from ethyl acetate or acetonitrile. The higher yields, relative ease of purification and abundance of commercially available aldehydes make Method B desirable for large-scale preparation and rapid analysis of structure–activity relationships of 2-substituted analogues. The parent compound (**5a**, R = H) was initially synthesized as well as several aryl- and heteroaryl analogues (**5f–q**). A similar transformation from phenylene diamines to benzimidazoles was undertaken in previous publications using Cu(OAc)<sub>2</sub>.<sup>20,26</sup> This method, while affording the desired benzimidazoles in moderate yields, the workup requires subjecting the compounds to strongly acidic and basic conditions. The workup for method B is much milder and requires just a simple filtration and recrystallization in many instances.

Substituted aryl derivatives were synthesized to determine simple structure–activity relationships around the phenyl ring of compound **5c**. Phenyl substituted analogues **5m–q** were prepared by the route outlined in Scheme 1 (Method B) in yields ranging from 32 to 82%. The *ortho*-, *meta*- and *para*-methyl derivatives **5m**, **5n** and **5o** were synthesized to determine the effect of simple aryl substitution on enzyme activity. Further derivatization from the 3- and 4-positions was performed to incorporate tertiary amines in the compounds for salt formation and improved physiologic solubility. Other amine salts **11a–b** were synthesized by the coupling of carboxylic acid **5p** with *N*-methylpiperazine and *N,N,N*-trimethylpropylenediamine in dichloromethane in



**Scheme 1.** (a) Toluene/SOCl<sub>2</sub>, MeOH, 95%; (b) ethylenediamine, NaHCO<sub>3</sub>, *n*BuOH, 84%; method A: (c) THF, RC(O)Cl, Et<sub>3</sub>N, 30–87%; (d) H<sub>2</sub>, 50 psi, Pd/C, MeOH, quant; (e) toluene reflux, 3 days, 30–55%; method B: (f) Raney Ni, H<sub>2</sub>NNH<sub>2</sub>, MeOH, 94%; (g) RCHO, Pd/C, MeOH, 30–82%.



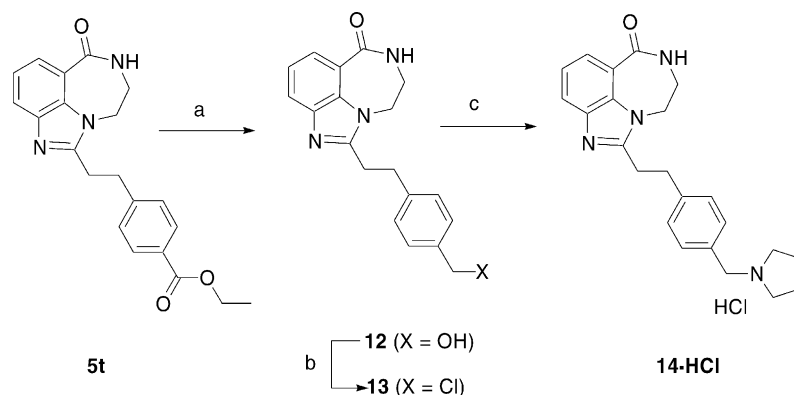
**Scheme 2.** Method C: (a) EDC/DMAP, DCM/NMP, HNR<sub>2</sub>, 51–91% yield; (b) 2.0 M HCl/Et<sub>2</sub>O (xs), quant.

excellent yields (Method C, **Scheme 2**). The salt formation of **5q** and **11a–b** was accomplished by suspending the free base in ethyl acetate followed by the addition of hydrochloric acid (2.0 M in diethyl ether) in order to quantitatively precipitate the HCl salt out of solution.

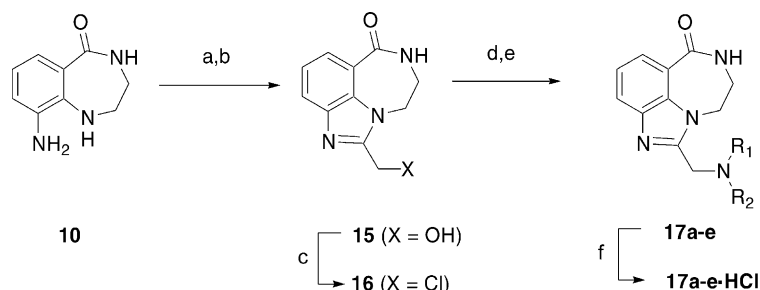
Similarly, the phenethyl substituted derivatives of **5g** were synthesized as outlined in **Scheme 3**. Compounds

**5r**, **5s** and **5t** were formed by the addition of diamine **10** to the requisite aldehydes as illustrated in **Scheme 1** (Method B) in yields ranging from 35 to 82%. The alcohol **12** was synthesized from the ester **5t** by reduction with lithium aluminum hydride in 96% yield. Further chlorination of the alcohol **12** with thionyl chloride afforded benzylic chloride **13** in 72% yield. Amination with pyrrolidine directly formed the water-soluble amine hydrochloride salt **14·HCl**.

Using tertiary amines as a means to make physiologically soluble salts led to the synthesis of derivatives **17a–e** (**Scheme 4**). For the preparation of amines **17a–e**, the route outlined in **Scheme 4** was utilized. The diamine **10** reacted with the commercially available *t*-butyldimethylsilyloxyacetaldehyde in THF to yield the alcohol **15** after deprotection with TBAF. The chlorination of alcohol **15** with thionyl chloride led to the chloride **16** in 74% yield. Amination of chloride **16** in acetonitrile resulted in amines **17a–e** in yields ranging from 69–89%. The salt forms of these amine derivatives (**17a–e·HCl**) were synthesized by simple protonation with hydro-



**Scheme 3.** (a) LAH, THF, 96%; (b) SOCl<sub>2</sub>, 72%; (c) pyrrolidine, CH<sub>3</sub>CN, 92%.



**Scheme 4.** (a) TBDMISOCH<sub>2</sub>CHO, Pd/C, MeOH, 76%; (b) TBAF, 89%; (c) SOCl<sub>2</sub>, 74%; (d) HNR<sub>2</sub>, K<sub>2</sub>CO<sub>3</sub>, CH<sub>3</sub>CN; (e) HCl/Et<sub>2</sub>O (2.0 M), EtOAc or CH<sub>3</sub>CN, 69–89%; (f) 2.0 M HCl/Et<sub>2</sub>O, quant.

chloric acid and precipitation from ethyl acetate or acetonitrile.

### Biological Evaluation and SAR Discussion

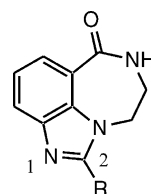
Table 1 summarizes the basic differences in potency between the benzodiazepines, imidazobenzodiazepines and other classes of PARP-1 inhibitors. As stated in the introduction, the ‘first-generation’ PARP-1 inhibitor, 3-aminobenzamide (3-AB, R = NH<sub>2</sub>, **1a**) displays a modest potency against the enzyme (IC<sub>50</sub> = 9.8 μM). One member of the ‘second-generation’ PARP-1 inhibitors, 5-nitroisoquinolin-1-one **2a** (IC<sub>50</sub> = 3.4 μM) displays enzymatic activity 3 times better than 3-AB. 5-Aminoisoquinolin-1-one **2b** (IC<sub>50</sub> = 300 nM)<sup>27</sup> is one of the most potent members of this series emphasizing the importance of the amine in the 5-position. Based on crystallographic data, this amine is in a position to form a water-mediated H-bond with PARP-1, accounting for enhanced potency.<sup>20</sup>

The potency of the seven-membered nitro benzodiazepine **8** (entry 4) was similar to the 5-nitroisoquinolin-1-one **2a**. The aminobenzodiazepine **10**, however, did not improve to the same degree as **2b** underscoring the necessity of both a planar, fused ring system (isoquinolone) and the amine in the 5-position for inhibition. Improvement to the benzodiazepine core did occur, however, by fusing a five-membered ring to this moiety leading to the imidazobenzodiazepine **5a** (IC<sub>50</sub> = 299 nM). Similar to **2b**, the imidazobenzodiazepine core has three key elements that contribute to the overall potency: (1) the conformationally constrained

benzamido moiety (2) the planar, fused ring system (benzimidazole) and (3) the N1 nitrogen that can form a water-mediated H-bond to the enzyme as discussed in the molecular modeling section. To reiterate, the resulting imidazobenzodiazepine core **5a** is an order of magnitude more potent than benzamide **1**, isoquinolone **2a**, and benzodiazepines **8** and **10**. Compound **5a** also displays similar potency to the compounds in other series of PARP-1 inhibitors, namely isoquinolones **2b**, 5[*H*]-phenanthridin-6-one **3**, benzimidazole **4a**, and tricyclic indole **4c** (Table 1, entries 7–9).

Outlined in Table 2 are the activities of several 2-substituted derivatives of the imidazobenzodiazepine core, such as methyl derivative **5b** (entry 2)<sup>28</sup> as well as several aryl- and heteroaryl compounds. The addition of aryl groups at the 2-position maintained or improved activity over **5a** in almost every instance. The 2-phenyl (**5c**, entry 3), 2-(*m*-pyridyl) (**5j**, entry 10), and 2-furyl (**5k**, entry 11), derivatives had slightly better activity than the core **5a**, while the pyrrolyl (**5l**, entry 12) and β-naphthyl derivatives (**5e**, entry 5) were 5 and 9 times as potent, respectively.

**Table 2.** PARP-1 inhibition of 2-substituted imidazobenzodiazepines



Entry	Compd	R group	Method <sup>a</sup>	Yield (%)	IC <sub>50</sub> (nM)
1	<b>5a</b>	H	B	32	299
2	<b>5b</b>	CH <sub>3</sub>	A	49 <sup>b</sup>	141
3	<b>5c</b>	Ph	A	40 <sup>b</sup>	90
4	<b>5d</b>	α-Np	A	43 <sup>b</sup>	382
5	<b>5e</b>	β-Np	A	55 <sup>b</sup>	32
6	<b>5f</b>	CH <sub>2</sub> Ph	B	52	108
7	<b>5g</b>	CH <sub>2</sub> CH <sub>2</sub> Ph	B	76	26
8	<b>5h</b>	( <i>E</i> )-CH=CHPh	B	75	71
9	<b>5i</b>	C≡;CPh	B	75	44
10	<b>5j</b>	3-Pyridyl	B	54	168
11	<b>5k</b>	2-Furyl	B	75	108
12	<b>5l</b>	2-Pyrrolyl	B	48	61
13	<b>17a</b>	-CH <sub>2</sub> N(CH <sub>3</sub> ) <sub>2</sub>		42 <sup>c</sup>	66

**Table 1.** PARP-1 inhibition for several classes of PARP-1 inhibitors

Entry	Compd	IC <sub>50</sub> (μM) <sup>a</sup>
1	<b>1a</b>	9.8
2	<b>2a</b>	3.4
3	<b>2b</b>	0.3
4	<b>8</b>	5.1
5	<b>10</b>	2.6
6	<b>5a</b>	0.299
7	<b>4a</b>	0.750 <sup>b</sup>
8	<b>4c</b>	0.203 <sup>c</sup>
9	<b>3</b>	0.340

<sup>a</sup>See Experimental for details.

<sup>b</sup>Compound synthesized as indicated in ref 21.

<sup>c</sup>Compound synthesized as indicated in ref 24.

<sup>a</sup>See Experimental for details.

<sup>b</sup>Yield from compound **8**.

<sup>c</sup>See Scheme 4, overall yield from **10**.

This result concurs with findings by other groups indicating that the most potent (<100 nM) PARP-1 inhibitors have multiple aromatic rings within their structures, similar to these derivatives.<sup>23,24</sup> In fact, the only aromatic moiety that decreased the core activity was the  $\alpha$ -naphthyl group (**5d**,  $IC_{50}$  = 382 nM). In compound **5d**, however, the naphthyl ring is more orthogonal to the core than in any other aryl derivative, thus disrupting the planarity of the inhibitor.

Remarkable improvements in activity also occurred by the addition of two atoms between the 2-position of the imidazobenzodiazepine core and aryl group. While the extension of the aryl moiety by one methylene unit showed some improvement, as compared to the core activity (**5f**, entry 6), the addition of two carbon atoms between the core and the aryl ring led to three of the most active compounds in the series (**5g–i**, entries 7–9) as discussed *vide infra*. Also, the addition of a tertiary amine to the 2-position resulted in compound **17a** whose activity, despite the lack of an aryl substituent is similar to the best compounds within the series (Table 2, entry 13), necessitating further derivatization.

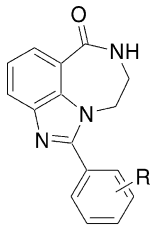
The inhibitory activities of aryl-substituted derivatives of **5c** are outlined in Table 3. In general, substitution at the *ortho*-position of the aryl ring, as foreshadowed by the poor activity of  $\alpha$ -naphthyl analogue **5d**, was more deleterious to activity than either the *meta*- or *para*-substitution. Compound **5m** was approximately three times less active than the parent phenyl derivative **5c**, while the isomeric tolyl derivatives **5n** and **5o** (Table 3, entries 3 and 4) displayed similar potencies to this core. With these data in mind, solubilizing groups were appended to the 3- and 4-positions of the phenyl ring. The amides **11a** and **11b** (Table 3, entries 6–7) as well as

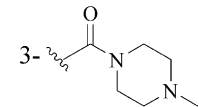
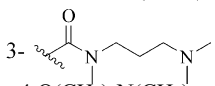
their synthetic precursor **5p** (Table 3, entry 5) demonstrated a slightly weaker potency than **5c**, but they have the added benefit of a water-solubilizing group (tertiary amine and carboxylic acid). The *para*-substituted compound **5q** (Table 3, entry 8,  $IC_{50}$  = 63 nM), however, was more potent than any phenyl substituted derivative. The potency of **5q** and the potential to form a water-solubilizing salt prompted further *in vivo* studies for this compound as discussed below. Compounds **11a–b** and **5q** further demonstrate that there is minimal loss in potency even with large, hydrophobic groups at the 2-position.

The *in vitro* PARP-1 inhibition results from the derivatives of **5g** are outlined in Table 4. There was a notable decline in activity upon derivatization of the two-carbon linker. The addition of a methyl group reduced the activity several fold (Table 4, entry 2) as did the addition of an amine (Table 4, entry 3). Derivatization of the aryl ring of **5g** also resulted in a moderate reduction in activity in almost every instance. Hydrophilic groups in the *para* position, however, were more deleterious to activity than hydrophobic ones. For example, the carboxylic acid **5u**, and the alcohol **12** were an order of magnitude worse than **5g** (Table 4, entries 5 and 6) while the more hydrophobic ester **5t** and amine **14·HCl** showed comparable activity to **5g** (Table 4 entries 4 and 7).

The PARP-1 *in vitro* potencies of amine derivatives **17a–e** are outlined in Table 5. Once again, this series of compounds illustrates the tolerance that the enzyme has for large, hydrophobic groups. Minimal loss in activity from **17a** is noted with the *N*-methyl-*N*-benzyl and bicyclic derivatives **17b** and **17e** (Table 5, entries 2 and 5). Even the bulky *t*-butyl ester derivative **17d** (Table 5, entry 4) is only 3 times worse than **17a**.

Table 3. PARP-1 inhibition of analogues of **5c**

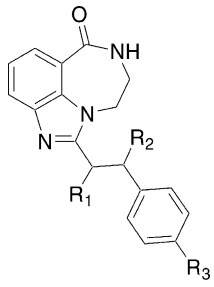


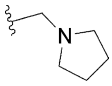
Entry	Compd	R group	Method <sup>a</sup>	Yield (%)	$IC_{50}$ (nM)
1	<b>5c</b>	H	A	40	90
2	<b>5m</b>	2-CH <sub>3</sub>	B	32	329
3	<b>5n</b>	3-CH <sub>3</sub>	B	45	97
4	<b>5o</b>	4-CH <sub>3</sub>	B	69	111
5	<b>5p</b>	3-COOH	B	82	155
6	<b>11a</b>	3- 	C	91 <sup>b</sup>	161
7	<b>11b</b>	3- 	C	51 <sup>b</sup>	244
8	<b>5q</b>	4-O(CH <sub>2</sub> ) <sub>3</sub> N(CH <sub>3</sub> ) <sub>2</sub>	B	65	63

<sup>a</sup>See Experimental for details.

<sup>b</sup>Yield from coupling reaction in Scheme 2.

Table 4. PARP-1 inhibition of analogues of **5g**<sup>d</sup>



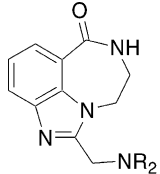
Entry	Compd	R <sub>1</sub>	R <sub>2</sub>	R <sub>3</sub>	Yield (%)	$IC_{50}$ (nM)
1	<b>5g</b>	H	H	H	76 <sup>a</sup>	26
2	<b>5r(±)</b>	H	CH <sub>3</sub>	H	35 <sup>a</sup>	130
3	<b>5s(S)</b>	NH <sub>2</sub>	H	H	47 <sup>b</sup>	183
4	<b>5t</b>	H	H	COOEt	82 <sup>a</sup>	97
5	<b>12</b>	H	H	CH <sub>2</sub> OH	96 <sup>c</sup>	284
6	<b>5u</b>	H	H	COOH	82 <sup>a</sup>	259
7	<b>14·HCl</b>	H	H		92	68

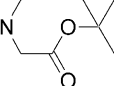
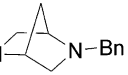
<sup>a</sup>Method B was used.

<sup>b</sup>Yield after deprotection.

<sup>c</sup>Yield after reduction of **5t**.

<sup>d</sup>Yield from amination of **13**.

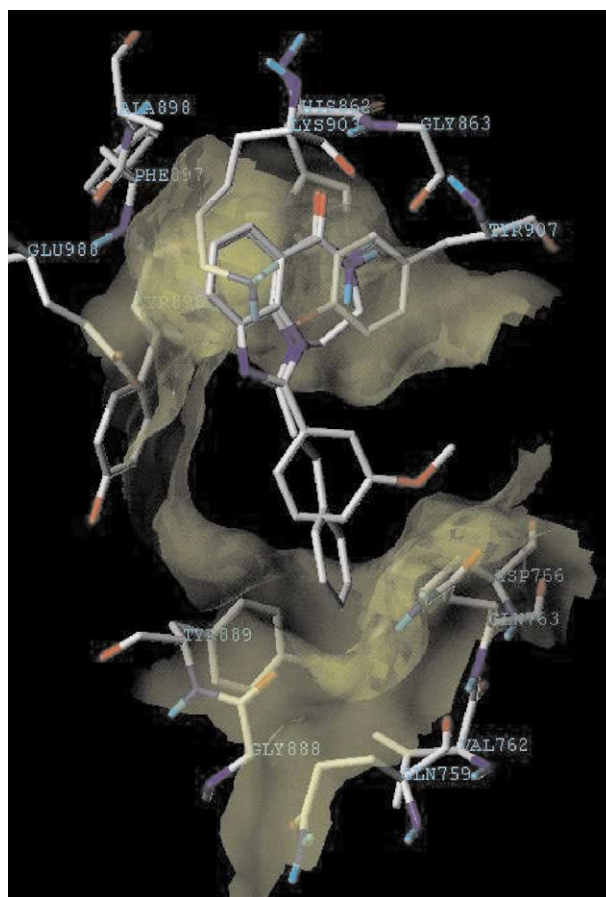
**Table 5.** PARP-1 inhibition of analogues of **17a**


Entry	Compd	NR <sub>2</sub>	Yield (%) <sup>a</sup>	IC <sub>50</sub> (nM) <sup>b</sup>
1	<b>17a</b>		82	66
2	<b>17b</b>		74	88
3	<b>17c</b>		72	109
4	<b>17d</b>		70	187
5	<b>17e</b>		82	74

<sup>a</sup>Represents yield from chloride **16**.<sup>b</sup>See Experimental for details.

### Molecular Modeling Data

Most of the SAR obtained from the compounds in Tables 1–5 can be explained with the aid of computer modeling and the published crystal structure data.<sup>20,24</sup> We modeled compound **5g** with benzimidazole **4b** (R = 3-methoxyphenyl) to illustrate the key interaction between the substituent on the 2-position of the imidazole ring and the enzyme. The nicotinamide binding pocket presumably binds the amide moiety in compound **5g** in an analogous manner to the primary amide in the benzimidazole **4b** (fig. 2). This portion of the pocket contains one hydrogen bond from Ser904 and two hydrogen bonds from Gly863 to the amide oxygen and nitrogen. This binding conformation is widely accepted and provides the primary ‘signature’ element for PARP-1 inhibitors as defined by previous studies where the amide is altered or deleted.<sup>20,24</sup> There is also a propensity for planar compounds to bind in the active site of PARP-1.<sup>29</sup> This fact can be explained by the position of two parallel tyrosine residues (Tyr896 and Tyr907) that are within the active site. These two tyrosine residues interact with the planar aryl moieties of many PARP-1 inhibitors by forming a  $\pi$ -electron ‘sandwich’. This pi stacking is beneficial for binding planar aromatic compounds.<sup>30,31</sup> This planar pocket is utilized by 2-aryl and 2-heteroaryl substituted imidazobenzodiazepines (e.g., **5c**, **5e** and **5j–l**), accounting for their potency. Compounds **5g–i** can utilize a secondary interaction with the hydrophobic pocket formed by residues Tyr889, Gly888, and Val762. Any substitution on the aryl ring of **5g** (R<sub>3</sub>) presumably forces this aryl ring out of this secondary binding pocket, resulting in a higher IC<sub>50</sub> (e.g., **5t**, **5u**, **12** and **14**, Table 4). In addition, this pocket could explain the increased activity of naphthyl derivative **5e** over its isomer **5d**, whose naphthyl side chain is unable to access this pocket.

**Figure 2.** Molecular model of **5g** and benzimidazole **4b** in the PARP-1 catalytic site.

### Pharmacology Data

#### Caco-2 data

In order to further probe the drug-like characteristics of this series of PARP-1 inhibitors, representative compounds from various subseries (**5g**, **5k**, **5q** and **17a**) were tested for permeability using the caco-2 cell model.<sup>32</sup> In this model, the concentration of compound is measured both apically and basolaterally in caco-2 intestinal cells to determine the propensity for passive diffusion and/or active transport. The permeability ratio is determined for diffusion/transport in each direction (basolateral to apical, B–A cm/s $\times 10^6$  and apical to basolateral, A–B cm/s $\times 10^6$ ) and the ratio of these two results is indicated in Table 6 as the efflux ratio. As shown in Table 6, compounds **5g**, **5k**, **5q** and **17a** are all highly permeable (> 10 cm/s $\times 10^{-6}$ ).<sup>33</sup> In addition, none of the imidazobenzodiazepines tested were high-risk efflux substrates as indicated by the ratio of permeability measurements (high-risk substrates: efflux ratio > 10).

These Caco-2 results predict that imidazobenzodiazepines are highly permeable and at low risk for efflux. The hydrophobic nature of this class of compounds is similar to that of most PARP-1 inhibitors, thus one would predict comparable permeability profiles with other classes as indicated by 5[*H*]-phenanthridin-6-one **3** (entry 5).

**Table 6.** Caco-2 permeability results<sup>a</sup>

Entry	Compd	Permeability B–A <sup>b</sup> (cm/s×10 <sup>-6</sup> )	Permeability A–B <sup>b</sup> (cm/s×10 <sup>-6</sup> )	Efflux Ratio <sup>c</sup>
1	<b>5g</b>	46.2	65.4	1.42
2	<b>5k</b>	34.4	64.0	1.86
3	<b>5q</b>	20.7	46.9	2.27
4	<b>17a</b>	10.3	18.0	1.75
5	<b>3</b>	36.3	72.9	2.01

<sup>a</sup>See ref 32 for experimental details.

<sup>b</sup>High permeability: > 10 cm/s×10<sup>-6</sup>; medium permeability: 1–10 cm/s×10<sup>-6</sup>; low permeability: < 1 cm/s×10<sup>-6</sup>. See ref 33.

<sup>c</sup>High-risk efflux substrate has ratio > 10. See ref 33.

### Streptozotocin-induced diabetic mice data

Previous studies indicate that PARP-1 is involved with the regeneration of  $\beta$ -islet cells in the pancreas and consequently delay or even reverse the progression of type 1 *Diabetes mellitus*.<sup>7</sup> Streptozotocin (STZ) is a chemical that specifically damages islet  $\beta$ -islet cells in the pancreas ultimately leading to the development of type 1 diabetes in mice. This model was utilized to demonstrate the in vivo efficacy of PARP-1 inhibitors to attenuate the hyperglycemia. In this model, the compounds were administered ip (or orally for **17a**) prior to insult with streptozotocin. Compounds **5q**, **17a** and **17e** were pre-administered to STZ induced diabetic mice and the blood glucose levels were monitored over several hours. The administration of **5q**, **17a**, and **17e** at 10 mg/kg resulted in a 67–75% reduction of the hyperglycemia (Table 7, entries 3–5) compared to the vehicle treated animals (no STZ, Table 7, entry 1). That is, *diabetic mice treated with PARP-1 inhibitors recovered 67–75% of their normal glucose levels*. The higher dose (30 mg/kg) of these compounds resulted in a comparable reduction while the lowest dose (3 mg/kg) was ineffective. Perhaps the most interesting result from this study is that *compound 17a even showed moderate efficacy when administered orally* (Table 7, entry 6).

### Focal cerebral ischemic stroke data

As PARP-1 activation is implicated in the pathogenesis of stroke, preliminary data was obtained on PARP-1 inhibitors in two models of stroke, a transient<sup>34</sup> and a permanent middle cerebral areterial occlusion model.<sup>35</sup> In the transient model, rats were injected with 20 mg/kg

**Table 7.** Percent reduction of blood glucose levels in STZ induced mice<sup>a</sup>

Entry	Compd	3 mg/kg	10 mg/kg	30 mg/kg
1	Vehicle (no STZ)	100	100	100
2	STZ control	0	0	0
3	<b>5q</b> <sup>b</sup>	26.6	67.2	72.8
4	<b>17e</b> <sup>b</sup>	12.5	72.7	78.1
5	<b>17a</b> <sup>b</sup>	46.1	74.8	83.2
6	<b>17a</b> <sup>c</sup>	29.2	62.4	69.3

<sup>a</sup>See ref 40 for experimental details.

<sup>b</sup>Drug was administered ip.

<sup>c</sup>Drug was administered orally.

of **5g** ip 30 min pre occlusion. Then, 30 min after ischemia, 20 mg/kg **5g** was given as a bolus dose ip. After sacrifice at 24 h, the resulting tissue slices indicated a 59% reduction in infarct volume (Table 8, entry 1). *This reduction compares favorably with the best known PARP-1 inhibitor reported in the literature*.<sup>19</sup> *In a somewhat more stringent model of stroke, the permanent cerebral ischemic model, 5g also demonstrated a remarkable neuroprotective effect*. Compound **5g** reduced infarct volume by 39% (entry 2, Table 8) when administered in rats where the middle cerebral artery was permanently occluded.

As stated above, ischemic diseases should ideally be treated by iv administration of the drug and results from iv administered PARP-1 inhibitors in animal models will be reported in due course.

### Conclusions

We have designed and synthesized a series of 2-substituted imidazobenzodiazepines as potent PARP-1 inhibitors with clearly defined structure–activity relationships. This new series includes several examples of highly potent PARP-1 inhibitors (10 examples, 26–100 nM). Molecular modeling accounts for the potencies of the most active compounds in vitro as illustrated by an additional binding pocket for the side chains of compounds **5e** and **5g–i**. Representative examples from each subseries were determined to be highly permeable. Finally and most importantly, this series of PARP-1 inhibitors demonstrates activity in vivo as compounds **5q**, **17a** and **17e** showed prominent reduction of hyperglycemia in the mouse streptozotocin induced diabetes model and compound **5g** displayed a significant neuroprotective effect in the rat transient and permanent MCAO model of brain ischemia.

### Experimental

#### General

Melting points were obtained on a MEL-TEMP II (Meltemp Laboratory Devices, Inc.). Proton nuclear magnetic resonance were recorded at 400 MHz on a Varian 400 using deuterated solvent as an internal standard. Chemical shift values are indicated in parts per million. Mass spectra were recorded using a Micromass LCS Platform LC/MS. Elemental analyses were obtained from Atlantic Microlabs, Inc.

**Table 8.** Cerebral ischemic stroke results

Entry	Compound	Dose (mg/kg)	Reduction in infarct volume	MCAO model
1	<b>5g</b>	40 <sup>a</sup>	59 ( $r=0.009$ )	Transient <sup>b</sup>
2	<b>5g</b>	40 <sup>a</sup>	39 ( $r=0.02$ )	Permanent <sup>c</sup>

<sup>a</sup>Compound was administered 20 mg/kg, 30 min pre-occlusion and 20 mg/kg 30 min post-ischemia.

<sup>b</sup>See ref 34.

<sup>c</sup>See ref 35.

(Norcross, GA, USA). All reagents were purchased from Aldrich Chemical (Milwaukee, WI, USA) unless otherwise stated.

**Synthesis of 9-nitro-1,2,3,4-tetrahydro-benzo[e][1,4]diazepin-5-one (8)** 2-Chloro-3-nitro-benzoic acid methyl ester **7** (1.0 g, 4.7 mmol), prepared from 2-chloro-3-nitro-benzoic acid **6** according to literature,<sup>36</sup> was dissolved in *n*-butanol (5 mL). Sodium carbonate (0.50 g, 4.7 mmol) was added to the solution followed by ethylene diamine (282 mg, 4.7 mmol). After several h of heating at 80 °C, an orange solid started to precipitate out of solution. The reaction was stopped after 16 h and the orange solid was filtered off and washed with water several times and recrystallized from EtOAc. The dry yield of the final orange crystals was 810 mg (84%). mp = 187–190 °C (dec). <sup>1</sup>H NMR (DMSO-*d*<sub>6</sub>) δ 8.72 (t, 1H), 8.42 (t, 1H), 8.23 (d, 1H), 8.15 (d, 1H), 6.75 (t, 1H), 3.64 (m, 2H), 3.35 (m, 2H). Anal. calcd for C<sub>9</sub>H<sub>9</sub>N<sub>3</sub>O<sub>3</sub>: C, 52.17; H, 4.38; N, 20.28. Found: C, 52.25; H, 4.59; N, 20.19.

#### Method A

**General procedure for the acylation of 8.** A solution of compound **8** (460 mg, 2.22 mmol) was dissolved in THF (10 mL). Triethyl amine (340 μL, 2.44 mmol) was added to this solution followed by acetyl chloride (175 μL, 2.44 mmol). The solution was stirred overnight with gentle warming (50 °C). The reaction was quenched with water (10 mL) followed by extraction with EtOAc (3 × 10 mL). The combined organics were dried, concentrated and chromatographed on silica gel to yield compound **9b** in 30% yield (160 mg).

**1-Acetyl-9-nitro-1,2,3,4-tetrahydro-benzo[e][1,4]diazepin-5-one (9b)** <sup>1</sup>H NMR (CDCl<sub>3</sub>) δ 8.13 (d, 1H), 8.06 (d, 1H), 7.72 (t, 1H), 6.96 (t, 1H), 4.97 (m, 2H), 3.36 (m, 2H), 2.25 (s, 3H). This material was used without further purification.

**1-Benzoyl-9-nitro-1,2,3,4-tetrahydro-benzo[e][1,4]diazepin-5-one (9c)** Yield = 80%. <sup>1</sup>H NMR (CDCl<sub>3</sub>) δ 8.63 (bs, 1H), 8.40 (d, 1H), 8.06 (d, 1H), 7.60 (d, 2H), 7.52 (t, 1H), 7.42 (t, 2H), 6.85 (t, 1H), 4.29 (m, 2H), 3.84 (m, 2H).

**1-(Naphthalene-1-carbonyl)-9-nitro-1,2,3,4-tetrahydro-benzo[e][1,4]diazepin-5-one (9d)** Yield = 87%. <sup>1</sup>H NMR (CDCl<sub>3</sub>) δ 8.60 (bs, 1H), 8.36 (d, 1H), 8.04 (m, 1H), 7.91 (d, 1H), 7.85 (m, 2H), 7.50 (m, 2H), 7.44 (m, 2H), 6.77 (t, 1H), 4.45 (m, 2H), 3.93 (m, 2H).

**1-(Naphthalene-2-carbonyl)-9-nitro-1,2,3,4-tetrahydro-benzo[e][1,4]diazepin-5-one (9e)** Yield = 85%. <sup>1</sup>H NMR (CDCl<sub>3</sub>) δ 8.69 (bs, 1H), 8.41 (d, 1H), 8.17 (s, 1H), 8.03 (d, 1H), 7.87 (m, 3H), 7.54 (m, 3H), 6.85 (t, 1H), 4.34 (m, 2H), 3.89 (m, 2H).

**General procedure for the cyclization of amides 9b–e (5b).** The acetamide **9b** (100 mg, 0.40 mmol) was dissolved in a 1:1 mixture of EtOAc/MeOH (10 mL). This solution was degassed and added to a nitrogen contain-

ing Parr Bomb with 10% Pd/C (25 mg). This solution was hydrogenated at 30 psi for 4 h. The mixture was filtered through a plug of Celite<sup>®</sup> and concentrated. The crude material was dissolved in boiling toluene and refluxed for 12 h to induce cyclization. After cooling, the solution was concentrated and the product was recrystallized from EtOAc to yield 35 mg (44%) of the final product.

**1-Methyl-8,9-dihydro-7H-2,7,9a-triaza-benzo[cd]azulen-6-one (5b).** mp = > 300 °C (dec); <sup>1</sup>H NMR (DMSO-*d*<sub>6</sub>) δ 8.35 (bt, 1H), 7.79 (d, 1H), 7.73 (d, 1H), 7.25 (t, 1H), 4.28 (m, 2H), 3.58 (m, 2H), 2.53 (s, 3H). Anal. calcd for C<sub>11</sub>H<sub>11</sub>N<sub>3</sub>O: C, 62.84; H, 5.75; N, 19.99. Found: C, 62.43; H, 5.54; N, 19.43.

**1-Phenyl-8,9-dihydro-7H-2,7,9a-triaza-benzo[cd]azulen-6-one (5c).** Yield = 40%; mp = 253–257 °C; <sup>1</sup>H NMR (DMSO-*d*<sub>6</sub>) δ 8.48 (bt, 1H), 7.89 (m, 4H), 7.59 (m, 3H), 7.37 (t, 1H), 4.47 (m, 2H), 3.54 (m, 2H). Anal. calcd for C<sub>16</sub>H<sub>13</sub>N<sub>3</sub>O: C, 72.97; H, 4.98; N, 15.96. Found: C, 72.32; H, 5.06; N, 15.88.

**1-Naphthalen-1-yl-8,9-dihydro-7H-2,7,9a-triaza-benzo[cd]azulen-6-one (5d).** Yield = 43%; mp = 226–229 °C; <sup>1</sup>H NMR (DMSO-*d*<sub>6</sub>) δ 8.43 (t, 1H), 8.18 (d, 1H), 8.09 (d, 1H), 7.98 (m, 2H), 7.91 (d, 1H), 7.83 (d, 1H), 7.71 (t, 1H), 7.59 (m, 2H), 7.43 (t, 1H), 4.13 (m, 2H), 3.53 (m, 2H). Anal. calcd for C<sub>20</sub>H<sub>15</sub>N<sub>3</sub>O (0.25H<sub>2</sub>O): C, 75.57; H, 4.92; N, 13.22. Found: C, 75.46; H, 4.87; N, 13.19.

**1-Naphthalen-2-yl-8,9-dihydro-7H-2,7,9a-triaza-benzo[cd]azulen-6-one (5e).** Yield = 55%; mp = 261–265 °C; <sup>1</sup>H NMR (DMSO-*d*<sub>6</sub>) δ 8.52 (t, 1H), 8.47 (s, 1H), 8.11 (m, 2H), 8.03 (m, 2H), 7.95 (d, 1H), 7.91 (d, 1H), 7.65 (m, 1H), 7.40 (t, 1H), 4.59 (m, 2H), 3.57 (m, 2H). Anal. calcd for C<sub>20</sub>H<sub>15</sub>N<sub>3</sub>O (1H<sub>2</sub>O): C, 72.49; H, 5.14; N, 12.68. Found: C, 72.23; H, 5.17; N, 12.65.

**Synthesis of 9-amino-1,2,3,4-tetrahydro-benzo[e][1,4]diazepin-5-one (10).** The nitro compound **8** (1.8 g, 8.7 mmol) was dissolved in MeOH (125 mL) and heated to 40 °C. Raney nickel (200 mg) was added to the solution followed by dropwise addition of hydrazine monohydrate (5 mL, xs). The reaction was heated to reflux for 30 min or until all of the starting material was gone. Then the mixture was filtered hot through a plug of Celite to remove the residual nickel. The Celite was washed with boiling MeOH (100 mL) and the filtrate was concentrated and dried in vacuo. The resulting air sensitive solid (1.45 g, 94%) was stored under nitrogen. An analytical sample of **10** could be obtained from trituration with diethyl ether. <sup>1</sup>H NMR (DMSO-*d*<sub>6</sub>) δ 7.91 (t, 1H), 7.03 (d, 1H), 6.69 (d, 1H), 6.47 (t, 1H), 4.97 (s, 2H), 4.64 (m, 2H), 3.20 (m, 2H). Anal. calcd for C<sub>9</sub>H<sub>11</sub>N<sub>3</sub>O (0.25H<sub>2</sub>O): C, 61.00; H, 6.26; N, 23.71. Found: C, 60.68; H, 6.29; N, 23.39.

#### Method B

**General procedure for synthesis of benzimidazoles 5a, f–q.** The diamine **10** (200 mg, 1.13 mmol), paraformaldehyde or desired aldehyde (1.1 equiv) and palladium on car-

bon (50 mg) were all mixed in MeOH (10 mL) and refluxed overnight. The reaction was filtered hot through a Celite plug and the filtrate was concentrated in vacuo. The resulting solid was triturated with diethyl ether or EtOAc (5 mL) and filtered. Analytical samples of the final products could be obtained by recrystallization in EtOAc or EtOAc/MeOH.

**8,9-Dihydro-7H-2,7,9a-triaza-benzo[cd]azulen-6-one (5a).** Yield = 32%; mp = 225–235 °C (dec); <sup>1</sup>H NMR (DMSO-*d*<sub>6</sub>) δ 8.45 (bt, 1H), 8.37 (s, 1H), 7.95 (m, 2H), 7.39 (t, 1H), 4.50 (m, 2H), 3.65 (m, 2H). Anal. calcd for C<sub>10</sub>H<sub>9</sub>N<sub>3</sub>O (0.75H<sub>2</sub>O) C, 59.84; H, 5.27; N, 20.94. Found: C, 59.69; H, 5.16; N, 20.73.

**1-Benzyl-8,9-dihydro-7H-2,7,9a-triaza-benzo[cd]azulen-6-one (5f).** Yield = 52%; mp = 224–227 °C; <sup>1</sup>H NMR (DMSO-*d*<sub>6</sub>) δ 8.53 (t, 1H), 8.02 (m, 2H), 7.47 (m, 6H), 4.51 (m, 2H), 3.75 (m, 2H), 2.70 (m, 2H). Anal. calcd for C<sub>17</sub>H<sub>15</sub>N<sub>3</sub>O (0.25H<sub>2</sub>O) C, 72.45; H, 5.54; N, 14.91. Found: C, 72.89; H, 5.55; N, 14.86.

**1-Phenethyl-8,9-dihydro-7H-2,7,9a-triaza-benzo[cd]azulen-6-one (5g).** Yield = 76%; mp = 195–200 °C; <sup>1</sup>H NMR (DMSO-*d*<sub>6</sub>) δ 8.37 (t, 1H), 7.86 (t, 2H), 7.34 (m, 3H), 7.25 (m, 3H), 4.22 (m, 2H), 3.55 (m, 6H). Anal. calcd for C<sub>18</sub>H<sub>17</sub>N<sub>3</sub>O: C, 74.20; H, 5.88; N, 14.42. Found: C, 73.05; H, 6.04; N, 14.49.

**(E)-1-Styryl-8,9-dihydro-7H-2,7,9a-triaza-benzo[cd]azulen-6-one (5h).** Yield = 75%; mp = 300–305 °C; <sup>1</sup>H NMR (DMSO-*d*<sub>6</sub>) δ 8.40 (t, 1H), 7.85 (m, 5H), 7.35 (m, 5H), 4.58 (m, 2H), 3.64 (m, 2H). Anal. calcd for C<sub>18</sub>H<sub>15</sub>N<sub>3</sub>O (0.1H<sub>2</sub>O) C, 74.26; H, 5.26; N, 14.43. Found: C, 74.17; H, 5.36; N, 14.38.

**1-Phenylethynyl-8,9-dihydro-7H-2,7,9a-triaza-benzo[cd]azulen-6-one (5i).** Yield = 75%; mp = 261–263 °C; <sup>1</sup>H NMR (DMSO-*d*<sub>6</sub>) δ 8.46 (t, 1H), 7.96 (d, 1H), 7.90 (d, 1H), 7.76 (d, 2H), 7.55 (m, 3H), 7.41 (t, 1H), 4.56 (m, 2H), 3.68 (m, 2H). Anal. calcd for C<sub>18</sub>H<sub>13</sub>N<sub>3</sub>O (0.3H<sub>2</sub>O) C, 73.86; H, 4.68; N, 14.35. Found: C, 73.92; H, 4.67; N, 14.27.

**1-Pyridin-3-yl-8,9-dihydro-7H-2,7,9a-triaza-benzo[cd]azulen-6-one (5j).** Yield = 54%; mp = 276–279 °C; <sup>1</sup>H NMR (DMSO-*d*<sub>6</sub>) δ 9.06 (s, 1H), 8.77 (d, 1H), 8.49 (t, 1H), 8.29 (d, 1H), 7.95 (d, 1H), 7.91 (d, 1H), 7.64 (t, 1H), 7.39 (t, 1H), 4.49 (m, 2H), 3.56 (m, 2H). Anal. calcd for C<sub>15</sub>H<sub>12</sub>N<sub>4</sub>O (0.25H<sub>2</sub>O): C, 67.03; H, 4.69; N, 20.84. Found: C, 67.07; H, 4.70; N, 20.71.

**1-Furan-2-yl-8,9-dihydro-7H-2,7,9a-triaza-benzo[cd]azulen-6-one (5k).** Yield = 75%; mp = 271–275 °C; <sup>1</sup>H NMR (DMSO-*d*<sub>6</sub>) δ 8.46 (t, 1H), 8.02 (s, 1H), 7.86 (d, 2H), 7.36 (t, 1H), 7.25 (d, 1H), 6.79 (d, 1H), 4.60 (m, 2H), 3.61 (m, 2H). Anal. calcd for C<sub>14</sub>H<sub>11</sub>N<sub>3</sub>O<sub>2</sub> (0.6H<sub>2</sub>O): C, 63.68; H, 4.66; N, 15.91. Found: C, 63.76; H, 4.54; N, 15.93.

**1-(1H-Pyrrol-2-yl)-8,9-dihydro-7H-2,7,9a-triaza-benzo[cd]azulen-6-one (5l).** Yield = 48%; mp = 323–330 °C; <sup>1</sup>H NMR (DMSO-*d*<sub>6</sub>) δ 11.93 (s, 1H), 8.45 (t, 1H), 7.79 (t,

2H), 7.31 (t, 1H), 7.04 (s, 1H), 6.77 (s, 1H), 6.29 (m, 1H), 4.53 (m, 2H), 3.59 (m, 2H); MS (ES+ = 253.21). Anal. calcd for C<sub>14</sub>H<sub>12</sub>N<sub>4</sub>O (0.4H<sub>2</sub>O): C, 64.80; H, 4.97; N, 21.59. Found: C, 64.78; H, 4.82; N, 21.75.

**1-o-Tolyl-8,9-dihydro-7H-2,7,9a-triaza-benzo[cd]azulen-6-one (5m).** Yield = 32%; mp = 224–229 °C; <sup>1</sup>H NMR (DMSO-*d*<sub>6</sub>) δ 8.47 (bt, 1H), 7.89 (m, 2H), 7.70 (s, 1H), 7.65 (d, 1H), 7.47 (t, 1H), 7.36 (m, 2H), 4.47 (m, 2H), 3.54 (m, 2H), 2.43 (s, 3H). Anal. calcd for C<sub>17</sub>H<sub>15</sub>N<sub>3</sub>O (0.5H<sub>2</sub>O): C, 72.68; H, 5.53; N, 14.96. Found: C, 72.88; H, 5.58; N, 14.91.

**1-m-Tolyl-8,9-dihydro-7H-2,7,9a-triaza-benzo[cd]azulen-6-one (5n).** Yield = 45%; mp = 234–238 °C; <sup>1</sup>H NMR (DMSO-*d*<sub>6</sub>) δ 8.47 (bt, 1H), 7.89 (m, 2H), 7.70 (s, 1H), 7.65 (d, 1H), 7.47 (t, 1H), 7.36 (m, 2H), 4.47 (m, 2H), 3.54 (m, 2H), 2.43 (s, 3H). Anal. calcd for C<sub>17</sub>H<sub>15</sub>N<sub>3</sub>O (0.5H<sub>2</sub>O): C, 72.68; H, 5.53; N, 14.96. Found: C, 72.88; H, 5.58; N, 14.91.

**1-p-Tolyl-8,9-dihydro-7H-2,7,9a-triaza-benzo[cd]azulen-6-one (5o).** Yield = 69%; mp = 258–263 °C; <sup>1</sup>H NMR (DMSO-*d*<sub>6</sub>) δ 8.44 (t, 1H), 7.88 (m, 2H), 7.76 (d, 1H), 7.37 (m, 3H), 4.45 (m, 2H), 3.53 (m, 2H), 2.42 (s, 3H). Anal. calcd for C<sub>17</sub>H<sub>15</sub>N<sub>3</sub>O: C, 73.63; H, 5.45; N, 15.15. Found: C, 73.13; H, 5.49; N, 15.10.

**3-(6-Oxo-6,7,8,9-tetrahydro-2,7,9a-triaza-benzo[cd]azulen-1-yl)-benzoic acid (5p).** Yield = 82%; mp = 300–320 °C; <sup>1</sup>H NMR (DMSO-*d*<sub>6</sub>) δ 13.28 (s, 1H), 8.48 (t, 1H), 8.41 (s, 1H), 8.11 (m, 2H), 7.90 (m, 2H), 7.72 (t, 1H), 7.37 (t, 1H), 4.47 (m, 2H), 3.54 (m, 2H). Anal. calcd for C<sub>17</sub>H<sub>13</sub>N<sub>3</sub>O<sub>3</sub> (0.25H<sub>2</sub>O) C, 65.48; H, 4.36; N, 13.48. Found: C, 65.46; H, 4.51; N, 13.43.

**General procedure for the coupling of acid 5p to amines (Method C).** Carboxylic acid **5p** (80 mg, 0.26 mmol), EDC (94 mg, 0.52 mmol), DMAP (5 mg) and the requisite amine (0.52 mmol) were mixed together in a solution of DCM/NMP (10:1, 5 mL). The reactions were agitated overnight. Workup consisted of washing with water (3 mL) and drying the organic phase through a plug of sodium sulfate. The crude amides **11a–b** were all isolated by concentrating the organic phase.

**1-[3-(4-Methyl-piperazine-1-carbonyl)-phenyl]-8,9-dihydro-7H-2,7,9a-triaza-benzo[cd]azulen-6-one (11a).** Yield = 91%; mp = 184–187 °C; <sup>1</sup>H NMR (DMSO-*d*<sub>6</sub>) δ 8.49 (bt, 1H), 7.90 (m, 4H), 7.67 (t, 1H), 7.58 (d, 1H), 7.38 (t, 1H), 4.49 (m, 2H), 3.65 (m, 2H), 3.55 (m, 2H), 3.35 (m, 2H), 2.35 (m, 4H), 2.20 (s, 3H). MS (ES+) = 389.98. Anal. calcd for C<sub>22</sub>H<sub>23</sub>N<sub>5</sub>O<sub>2</sub> (0.25H<sub>2</sub>O): C, 67.10; H, 6.05; N, 17.80. Found: C, 67.01; H, 6.04; N, 17.84. Salt formation of **11a·HCl** was done by suspending the free base in EtOAc and adding HCl/Et<sub>2</sub>O. The precipitate was filtered and washed with EtOAc to yield the purified salt. <sup>1</sup>H NMR (D<sub>2</sub>O) δ 7.75 (m, 3H), 7.60 (m, 3H), 7.32 (t, 1H, *J* = 8 Hz), 4.67 (m, 2H), 4.32 (m, 2H), 3.62 (m, 4H), 3.20 (m, 4H), 2.71 (s, 3H). Anal. calcd for C<sub>22</sub>H<sub>26</sub>ClN<sub>5</sub>O<sub>2</sub> (2H<sub>2</sub>O): C, 57.2; H, 6.10; N, 15.20. Found: C, 57.61; H, 6.03; N, 15.02.

***N*-(2-Dimethylamino-ethyl)-*N*-methyl-3-(6-oxo-6,7,8,9-tetrahydro-2,7,9a-triaza-benzo[*cd*]azulen-1-yl)-benzamide (11b).** Yield = 50%; <sup>1</sup>H NMR (DMSO-*d*<sub>6</sub>) δ 8.13 (d, 1H), 8.02 (d, 1H), 7.81 (m, 2H), 7.61 (m, 2H), 7.44 (t, 1H), 7.13 (t, 1H), 4.52 (m, 2H), 3.73 (m, 2H), 3.60 (m, 1H), 3.33 (m, 1H), 3.24 (m, 1H), 3.12 (s, 1.5H), 3.01 (s, 1.5H), 2.42 (m, 2H), 2.27 (s, 6H), 1.67 (m, 2H); MS (ES<sup>+</sup>) = 406.02. Anal. calcd for C<sub>23</sub>H<sub>27</sub>N<sub>5</sub>O<sub>2</sub>: C, 57.2; H, 6.10; N, 15.20. Found: C, 57.61; H, 6.03; N, 15.02. HCl salt of **11b**·HCl: <sup>1</sup>H NMR (D<sub>2</sub>O) δ 8.14 (t, 1H, *J* = 8 Hz), 8.07 (t, 1H, *J* = 8 Hz), 8.05 (s, 1H), 7.87 (m, 3H), 7.69 (t, 1H, *J* = 8 Hz), 4.66 (m, 2H), 3.77 (m, 4H), 3.37 (t, 2H, *J* = 8 Hz), 3.17 (s, 3H), 3.05 (s, 3H), 2.90 (s, 3H), 2.27 (m, 2H). Anal. calcd for C<sub>23</sub>H<sub>28</sub>ClN<sub>5</sub>O<sub>2</sub> (2.5H<sub>2</sub>O): C, 56.70; H, 6.81; N, 14.44. Found: C, 56.29; H, 6.78; N, 14.48.

**1-[4-(3-Dimethylamino-propoxy)-phenyl]-8,9-dihydro-7H-2,7,9a-triaza-benzo[*cd*]azulen-6-one (5q).** Yield = 65%; mp = 105–108 °C; <sup>1</sup>H NMR (CDCl<sub>3</sub>) δ 8.09 (d, 1H), 8.00 (d, 1H), 7.70 (d, 2H), 7.41 (t, 1H), 7.06 (d, 2H), 6.95 (bt, 1H), 4.50 (m, 2H), 4.11 (t, 2H), 3.73 (m, 2H), 2.52 (t, 2H), 2.30 (s, 6H), 2.02 (m, 2H). Anal. calcd for C<sub>21</sub>H<sub>24</sub>N<sub>4</sub>O<sub>2</sub> (1.5H<sub>2</sub>O): C, 64.43; H, 6.95; N, 14.31. Found: C, 64.74; H, 6.91; N, 14.15. **5q**·HCl: <sup>1</sup>H NMR (D<sub>2</sub>O) δ 7.69 (d, 1H), 7.65 (d, 1H), 7.29 (t, 1H), 7.25 (d, 2H), 6.68 (d, 2H), 4.50 (m, 2H), 4.05 (m, 2H), 3.64 (m, 2H), 3.24 (m, 2H), 2.88 (s, 6H), 2.12 (m, 2H). Anal. calcd for C<sub>21</sub>H<sub>24</sub>N<sub>4</sub>O<sub>2</sub> (1.0H<sub>2</sub>O, 1.0HCl): C, 60.73; H, 6.46; N, 13.49. Found: C, 60.80; H, 6.38; N, 13.37.

**1-(2-Phenyl-propyl)-8,9-dihydro-7H-2,7,9a-triaza-benzo[*cd*]azulen-6-one (5r).** Yield = 35%; mp = 163–167 °C; <sup>1</sup>H NMR (CDCl<sub>3</sub>) δ 8.04 (d, 1H), 7.93 (d, 1H), 7.36 (t, 1H), 7.23 (m, 4H), 7.11 (d, 1H), 6.91 (s, 1H), 3.90 (m, 1H), 3.60 (m, 1H), 3.42 (m, 1H), 3.01 (m, 1H) 1.75 (m, 2H), 1.48 (d, 3H). Anal. calcd for C<sub>19</sub>H<sub>19</sub>N<sub>3</sub>O (0.5 EtOAc): C, 72.18; H, 6.63; N, 12.03. Found: C, 71.73; H, 6.84; N, 12.15.

**(S)-1-(1-Amino-2-phenyl-ethyl)-8,9-dihydro-7H-2,7,9a-triaza-benzo[*cd*]azulen-6-one (5s).** The Boc protected amine was made by the general protocol of coupling *N*-Boc-L-phenylalanine carboxaldehyde with diamine **10**. Crude yield = 70%. The Boc group was deprotected by refluxing the crude carbamate in HCl/Et<sub>2</sub>O overnight. After stirring for 16 h, the solvent was removed and the residue was triturated with diethyl ether (1.0 M, 5 mL) and filtered. The crystals were washed several times with diethyl ether and dried to yield 405 mg (47%). Mp = 155–160 °C (dec.); <sup>1</sup>H NMR (DMSO-*d*<sub>6</sub>) δ 7.93 (d, 1H), 7.85 (d, 1H), 7.40 (t, 2H), 7.13 (m, 3H), 6.89 (d, 1H), 5.01 (m, 1H), 4.15 (m, 2H), 3.48 (m, 2H), 3.21 (t, 2H). Anal. calcd for C<sub>18</sub>H<sub>18</sub>N<sub>4</sub>O HCl (2H<sub>2</sub>O): C, 51.64; H, 5.86; N, 13.02. Found: C, 52.09; H, 5.74; N, 12.94.

**4-[2-(6-Oxo-6,7,8,9-tetrahydro-2,7,9a-triaza-benzo[*cd*]azulen-1-yl)-ethyl]-benzoic acid ethyl ester (5t).** Yield = 82%; mp = 230–233 °C; <sup>1</sup>H NMR (DMSO-*d*<sub>6</sub>) δ 8.34 (bt, 1H), 7.89 (d, 2H), 7.80 (m, 2H), 7.46 (d, 2H), 7.27 (t, 1H), 4.50 (m, 2H), 4.30 (q, 2H), 3.53 (m, 2H), 3.21 (m, 4H), 1.31 (t, 3H). MS (ES<sup>+</sup>) = 364.23. Anal. calcd for C<sub>21</sub>H<sub>21</sub>N<sub>3</sub>O<sub>3</sub> (0.25H<sub>2</sub>O): C, 68.56; H, 5.89; N, 11.42. Found: C, 68.30; H, 5.84; N, 11.52.

**4-[2-(6-Oxo-6,7,8,9-tetrahydro-2,7,9a-triaza-benzo[*cd*]azulen-1-yl)-ethyl]-benzoic acid (5u).** Yield = 82%; mp = 300–320 °C; <sup>1</sup>H NMR (DMSO-*d*<sub>6</sub>) δ 12.86 (bs, 1H), 8.35 (bt, 1H), 7.87 (d, 2H), 7.81 (m, 2H), 7.43 (d, 2H), 7.28 (t, 1H), 4.27 (m, 2H), 3.53 (m, 2H), 3.21 (m, 4H). Anal. calcd for C<sub>19</sub>H<sub>17</sub>N<sub>3</sub>O<sub>3</sub> (3H<sub>2</sub>O): C, 58.76; H, 4.71; N, 10.82. Found: C, 58.74; H, 4.85; N, 10.81.

**Reduction of ester 5w to form 1-[2-(4-hydroxymethyl-phenyl)-ethyl]-8,9-dihydro-7H-2,7,9a-triaza-benzo[*cd*]azulen-6-one (12).** Ethyl ester **5t** (500 mg, 1.38 mmol) was suspended in THF (20 mL) and cooled to 0 °C. Lithium aluminum hydride (100 mg, 2.74 mmol) was added portionwise over the next 30 min. The reaction mixture was stirred at room temperature overnight. The reaction was quenched with 10 mL EtOAc and washed with water (10 mL). The organic layer was partitioned and the aqueous layer was repeatedly extracted with EtOAc (4 × 10 mL). The combined organics were dried with Na<sub>2</sub>SO<sub>4</sub> and concentrated in vacuo. The resulting crude solid was triturated with diethyl ether (10 mL) and filtered. The resulting solid was characterized as the alcohol **12**. Yield = 400 mg (96%); <sup>1</sup>H NMR (DMSO-*d*<sub>6</sub>) δ 8.32 (bt, 1H), 7.78 (t, 2H), 7.25 (t, 1H), 7.22 (m, 4H), 5.11 (t, 1H), 4.45 (m, 2H), 4.44 (d, 2H), 3.49 (m, 2H), 3.12 (m, 2H), 3.08 (m, 2H); MS (ES<sup>+</sup>) = 322.40. Anal. calcd for C<sub>19</sub>H<sub>19</sub>N<sub>3</sub>O<sub>2</sub> (0.75H<sub>2</sub>O): C, 68.14; H, 6.08; N, 12.55. Found: C, 68.59; H, 6.08; N, 12.27.

**1-[2-(4-Chloromethyl-phenyl)-ethyl]-8,9-dihydro-7H-2,7,9a-triaza-benzo[*cd*]azulen-6-one (13).** The alcohol **12** (350 mg, 1.09 mmol) was added portionwise to a cooled (0 °C), stirred solution of thionyl chloride (3 mL). After 3 h of stirring, the thionyl chloride was removed in vacuo and the crude chloride was triturated with diethyl ether and filtered to yield 295 mg of the crude chloride (est purity > 95%). This material was aminated without further purification. <sup>1</sup>H NMR (DMSO-*d*<sub>6</sub>) δ 8.46 (bt, 1H), 7.88 (m, 2H), 7.35 (m, 4H), 4.74 (s, 2H), 4.30 (bs, 2H), 3.53 (bs, 2H), 3.27 (m, 2H), 3.17 (m, 2H); MS (ES<sup>+</sup>) = 340.30.

**Amination of chloride 13 to form 1-[2-(4-pyrrolidin-1-yl-methyl-phenyl)-ethyl]-8,9-dihydro-7H-2,7,9a-triaza-benzo[*cd*]azulen-6-one hydrochloride (14·HCl).** The benzyl chloride (850 mg, 2.5 mmol) was suspended in CH<sub>3</sub>CN with pyrrolidine (183 mg, 2.5 mmol) and heated to 60 °C overnight. After cooling the reaction mixture, the hydrochloride salt precipitated out and was filtered off to yield 950 mg (92%); <sup>1</sup>H NMR (D<sub>2</sub>O) δ 7.93 (d, 1H), 7.79 (d, 1H), 7.49 (t, 1H), 7.22 (d, 2H), 7.11 (d, 2H), 4.50 (m, 5H), 4.17 (s, 2H), 3.40 (m, 2H), 3.25 (m, 4H), 3.13 (m, 2H), 2.99 (m, 2H), 2.00 (m, 2H), 1.83 (m, 2H); MS (ES<sup>+</sup>) = 375.38. Anal. calcd for C<sub>23</sub>H<sub>27</sub>ClN<sub>4</sub>O<sub>1</sub> (4H<sub>2</sub>O): C, 57.19; H, 7.30; N, 11.60. Found: C, 56.93; H, 7.46; N, 11.74.

**Synthesis of 1-chloromethyl-8,9-dihydro-7H-2,7,9a-triaza-benzo[*cd*]azulen-6-one (16).** The amine **10** (12.5 g, 70.6 mmol), palladium on carbon (500 mg) and *t*-butyldimethylsilyloxyacetaldehyde (15.0 g, 84.7 mmol) were

suspended in 500 mL THF and refluxed overnight. The reaction was monitored by TLC (EtOAc) and after consumption of the amine (16 h), the palladium was filtered off and the filtrate was treated with tetrabutylammonium fluoride (75 mL, 1.0 M in THF). The solvent was removed and the resulting residue was triturated with 75 mL diethyl ether and 75 mL MeOH and filtered. The solid was dried and characterized as the intermediate alcohol **15** (13.6 g, 89%, >95% purity)  $^1\text{H NMR}$  (DMSO- $d_6$ )  $\delta$  8.37 (t, 1H), 7.82 (m, 2H), 7.29 (t, 1H), 5.64 (bs, 1H), 4.71 (s, 2H), 4.40 (m, 2H), 3.59 (m, 2H). This compound was chlorinated without further purification. The alcohol was added portionwise to thionyl chloride (25 mL) and stirred overnight. The thionyl chloride was then removed in vacuo and the residue was triturated several times with diethyl ether. The crude solid was recrystallized from acetonitrile (12.2 g, 74% overall yield).  $^1\text{H NMR}$  (DMSO- $d_6$ )  $\delta$  8.44 (t, 1H), 7.92 (d, 1H), 7.87 (d, 1H), 7.36 (t, 1H), 5.08 (s, 2H), 4.42 (m, 2H), 3.63 (m, 2H); MS (ES+ = 392.34). Anal. calcd for  $\text{C}_{11}\text{H}_{10}\text{ClN}_3\text{O}$ : C, 56.06; H, 4.28; N, 17.83. Found: C, 56.06; H, 4.27; N, 17.83. The amines **17a–e** were made from this compound.

**General procedure for amination of chloride 16. 1-Dimethylaminomethyl-8,9-dihydro-7H-2,7,9a-triaza-benzo[cd]azulen-6-one (17a).** The chloride **16** (775 mg, 3.3 mmol) was suspended in THF (20 mL) and dimethylamine (3.3 mL 2.0 M in THF, 6.6 mmol) was added followed by refluxing for 12 h. The solvent was removed in vacuo and the resulting solid was triturated with  $\text{H}_2\text{O}$  (10 mL) and filtered to yield the desired amine **17a** in 84% yield (675 mg).  $^1\text{H NMR}$  (DMSO- $d_6$ )  $\delta$  8.37 (t, 1H), 7.85 (d, 1H), 7.81 (d, 1H), 7.29 (d, 1H), 3.69 (s, 2H), 3.59 (m, 2H), 3.34 (s, 6H), 3.32 (m, 2H). Anal. calcd for  $\text{C}_{13}\text{H}_{16}\text{N}_4\text{O}$ : C, 63.92; H, 6.60; N, 22.93. Found: C, 63.55; H, 6.62; N, 22.42. The hydrochloride salt was prepared by suspending the amine in EtOAc (15 mL) followed by addition of 1.1 equiv HCl/Et $_2\text{O}$ . The reaction was stirred for 1 h followed by filtration and characterization of the HCl salt. **17a·HCl**:  $^1\text{H NMR}$  ( $\text{D}_2\text{O}$ )  $\delta$  8.02 (m, 2H), 7.51 (t, 1H), 4.82 (s, 6H), 4.76 (s, 2H), 4.50 (m, 2H), 3.81 (m, 2H). Anal. calcd for  $\text{C}_{13}\text{H}_{16}\text{N}_4\text{O}$  (0.8 $\text{H}_2\text{O}$ ): C, 52.90; H, 6.35; N, 18.98. Found: C, 53.11; H, 6.30; N, 19.03.

**1-(Benzyl-methyl-amino)-methyl-8,9-dihydro-7H-2,7,9a-triaza-benzo[cd]azulen-6-one (17b).** Yield = 72%; mp = 211–215 °C;  $^1\text{H NMR}$  (DMSO- $d_6$ )  $\delta$  8.44 (t, 1H), 7.89 (m, 2H), 7.35 (m, 6H), 4.45 (m, 2H), 3.90 (s, 2H), 3.65 (m, 2H), 3.62 (s, 2H), 2.17 (s, 3H); MS (ES+ = 321.01). Anal. calcd for  $\text{C}_{19}\text{H}_{20}\text{N}_4\text{O}$  (0.8 $\text{H}_2\text{O}$ ): C, 68.3; H, 6.45; N, 16.80. Found: C, 68.77; H, 6.23; N, 16.66.

**1-Pyrrolidin-1-ylmethyl-8,9-dihydro-7H-2,7,9a-triaza-benzo[cd]azulen-6-one (17c).** Yield = 74%; mp = 210–215 °C;  $^1\text{H NMR}$  (DMSO- $d_6$ )  $\delta$  8.37 (bt, 1H), 7.81 (m, 2H), 7.28 (t, 1H), 4.39 (bs, 2H), 3.88 (s, 2H), 3.58 (m, 2H), 3.35 (m, 4H), 1.70 (m, 4H). Anal. calcd for  $\text{C}_{15}\text{H}_{18}\text{N}_4\text{O}$  (1.0 $\text{H}_2\text{O}$ ): C, 62.5; H, 7.02; N, 19.49. Found: C, 62.22; H, 6.95; N, 19.60.

**[Methyl-(6-oxo-6,7,8,9-tetrahydro-2,7,9a-triaza-benzo[cd]azulen-1-ylmethyl)-aminol]-acetic acid tert-butyl ester (17d).** Yield = 70%; mp = 180–185 °C;  $^1\text{H NMR}$  (DMSO- $d_6$ )  $\delta$  8.37 (t, 1H), 7.82 (m, 2H), 7.29 (t, 1H), 4.48 (m, 2H), 3.94 (s, 2H), 3.58 (m, 2H), 3.26 (s, 2H), 2.30 (s, 3H), 1.38 (s, 9H). Anal. calcd for  $\text{C}_{18}\text{H}_{24}\text{N}_4\text{O}_3$ : C, 62.77; H, 7.02; N, 16.27. Found: C, 62.73; H, 7.05; N, 16.22.

**(S,S)-1-(5-Benzyl-2,5-diaza-bicyclo[2.2.1]hept-2-ylmethyl)-8,9-dihydro-7H-2,7,9a-triaza-benzo[cd]azulen-6-one (17e).** Yield = 82%; mp = 192–197 °C;  $^1\text{H NMR}$  ( $\text{CDCl}_3$ )  $\delta$  8.38 (t, 1H), 7.85 (d, 1H), 7.80 (d, 1H), 7.32 (m, 5H), 7.23 (m, 1H), 4.45 (m, 2H), 3.95 (dd, 2H), 3.65 (dd, 2H), 3.64 (m, 2H), 3.25 (m, 2H), 2.80 (m, 2H), 2.59 (m, 4H), 1.67 (m, 2H); MS (ES+) = 388.10. Anal. calcd for  $\text{C}_{23}\text{H}_{25}\text{N}_5\text{O}$ : C, 71.29; H, 6.50; N, 18.07. Found: C, 70.93; H, 6.40; N, 18.03. **17e·2HCl**:  $^1\text{H NMR}$  ( $\text{D}_2\text{O}$ )  $\delta$  7.98 (d, 1H), 7.89 (d, 1H), 7.52 (t, 1H), 7.45 (m, 5H), 4.43–4.18 (m, 6H), 3.83 (m, 2H), 3.72 (m, 2H), 3.63 (m, 2H), 3.32 (m, 2H), 3.03 (m, 2H), 2.25 (m, 2H). Anal. calcd for  $\text{C}_{23}\text{H}_{25}\text{N}_5\text{O}$ : C, 60.00; H, 5.91; N, 15.21. Found: C, 60.04; H, 6.06; N, 15.16.

**PARP-1 inhibition assay.** Purified recombinant human PARP from Trevigan (Gaithersburg, MD, USA) was used to determine the  $\text{IC}_{50}$  values of a PARP inhibitor. The PARP enzyme assay is set up on ice in a volume of 100  $\mu\text{L}$  consisting of 50 mM Tris-HCl (pH 8.0), 2 mM  $\text{MgCl}_2$ , 30  $\mu\text{g/mL}$  of DNase activated herring sperm DNA (Sigma, MO, USA), 30  $\mu\text{M}$  [ $^3\text{H}$ ]nicotinamide adenine dinucleotide (67 mCi/mmol), 75  $\mu\text{g/mL}$  PARP enzyme, and various concentrations of the compounds to be tested. The reaction was initiated by incubating the mixture at 25 °C. After 15 min of incubation, the reaction was terminated by adding 500  $\mu\text{L}$  of ice cold 20% (w/v) trichloroacetic acid. The precipitate formed is transferred onto a glass fiber filter (Packard Unifilter-GF/B) and washed three times with ethanol. After the filter is dried, the radioactivity is determined by scintillation counting.

#### Methods for molecular modeling

Three PARP-1 crystal structures (PDB designations: 1PAW,<sup>37</sup> 4PAX,<sup>30</sup> 1EFY<sup>20</sup>) were used as templates for molecular modeling. All modeling was performed using the Sybyl molecular modeling software (SYBYL 6.7.1 Tripos, Inc., St. Louis, MO 63144, USA). The MMFF94s forcefield was used for both the protein and ligand.<sup>38</sup> A distance dependent dielectric and 15 Å non-bonded cutoff were employed. The protein structure was held rigid during all calculations. Initial complex structures were obtained by overlaying the putative ligand onto the inhibitor from the 4PAX structure, requiring the crucial nicotinamide moiety to be conserved. Multiple conformations of each ligand were evaluated with each PARP crystal structure. From the initial complex structure, the ligand was minimized in the presence of the enzyme. Final structures were evaluated based on the number and quality of interactions made by the ligand with the protein. In most cases, the structures obtained using the 1PAW structure were deemed to be

superior. The location of the Gln763 sidechain in the 4PAX and 1EFY structures resulted in steric clashes between the inhibitor and the side chain of Gln763. In the 1PAW structure, the Gln763 sidechain is in a unique location resulting from a different conformation than observed in 4PAX and 1EFY. A small hydrophobic pocket is formed by the side chains of Val762, Gln763, Gln759 and Tyr889 in the 1PAW structure.

#### Methods for caco-2 permeability assay<sup>39</sup>

Caco-2 cells were grown at 37 °C in T-75 flasks in an atmosphere of 5% CO<sub>2</sub> and 95% relative humidity using Dulbecco's Modified Eagle's Medium (pH 7.4) supplemented with 10% fetal bovine serum, 1% non essential amino acids, and 0.05% penicillin–streptomycin. Cells were passaged at 80–90% confluency using a 0.25% trypsin/0.20% ethylene diamine tetraacetic acid (EDTA) solution. Media was changed approximately every 48 h. Caco-2 cells (passages 30–70) were seeded at 6.3 × 10<sup>4</sup> cells/cm<sup>2</sup> on polycarbonate 12-well Transwell<sup>®</sup> filters (Corning Costar Corporation, Cambridge, MA, USA) (3.0 μm mean pore size). Caco-2 cells were cultured on Transwells<sup>®</sup> under the same incubation conditions and used for transport experiments 21–28 days after seeding.

The permeability of PARP-1 inhibitors across Caco-2 cell monolayers was investigated (*n* = 3) in both apical to basolateral (AB) and basolateral to apical (BA) directions at donor concentrations of 100 mM. Permeability experiments were conducted at pH 7.0, 37 °C, 5% CO<sub>2</sub>, 95% relative humidity, and shaking at 50 revolutions per min (RPM) while maintaining sink conditions. Samples were collected at 30, 60 and 90 min and analyzed by HPLC/UV.

Permeability coefficients ( $P_{\text{eff}}$ ) of G0–G4 were calculated as previously reported. Control transport experiments were also conducted across Transwell<sup>®</sup> filters without Caco-2 cells to determine the filter permeability ( $P_{\text{filter}}$ ). The permeability of Caco-2 cell monolayers ( $P_{\text{m}}$ ) was estimated by correcting the effective permeability ( $P_{\text{eff}}$ ) for filter permeability ( $P_{\text{filter}}$ ) according to:  $P_{\text{eff}}^{-1} = P_{\text{m}}^{-1} + P_{\text{filter}}^{-1}$ .

#### Streptozotocin-induced diabetes assay

Male mice, (25–30 g, Charles River) were pre-treated with vehicle (DMSO, 2 mL/kg) or drug at 3, 10, 30, and 100 mg/kg ip, *n* = 5 in each group. After 30 min, acute hyperglycemia was induced by ip administration of streptozotocin (250 mg/kg, SIGMA-Aldrich, St. Louis, MO, USA).<sup>40</sup> After 48 h, blood glucose measurements were taken with a glucose test strip (Accu Check Advantage, Roche Diagnostics, New York, NY, USA). Two days after the STZ treatment, the blood glucose level in vehicle treated rats increases from a normal average of 140 – 460 ng/dl, a greater than 3-fold increase. The effect of drug pre-treatment is expressed as the percentage reduction in glucose level towards normal from the level measured in the vehicle-treated group. Statistical significance was determined using the

Student *t* test with a confidence interval accepted when  $p \leq 0.05$ .

#### Methods for testing 5g in focal cerebral ischemic stroke

**Transient MCAO model.** Transient focal ischemic stroke was modeled in rats using the intraluminal thread procedure as modified by Belayev.<sup>34</sup> Male Sprague–Dawley rats (280–320 g, Charles River, Wilmington, MA, USA) were anesthetized with isoflurane. A poly-lysinized 3–0 suture was inserted through the internal carotid artery into the origin of the middle cerebral artery (MCA). The suture is removed after 2 h of MCA occlusion.

**Permanent MCAO model.** Permanent focal cerebral ischemic stroke was modeled in rats using a modification of the method described by Chen et al.<sup>35</sup> Male Long Evans rats (280–350 g, Harlan–Sprague–Dawley, Indianapolis, IN, USA) were anesthetized with isoflurane. The right and left common carotid arteries and the right distal MCA were exposed and isolated. The distal MCA was cauterized and the carotids were transiently occluded for 90 min.<sup>41</sup>

All drugs were administered 30 min after the start of MCA occlusion. For both models, the brains were collected into cold PBS at 24 h after ischemia. The brains were sliced, processed for TTC histochemistry, and the infarcts were measured using computer-assisted planimetry. In the transient paradigm, total infarcts average 350 mm<sup>3</sup> including both cortical and subcortical tissue. In the permanent model, the infarcts were exclusively cortical and averaged 180 mm<sup>3</sup>. The effect of drug treatment is expressed as the percent reduction in infarct volume compared to coincident vehicle controls. Statistical significance was determined using the Student *t*-test with a confidence interval accepted when  $p \leq 0.05$ .

#### Acknowledgements

The authors thank Dr. Takashi Tsukamoto and Mr. Yao-Sen Ko for helpful comments regarding the manuscript.

#### References and Notes

- Decker, P.; Isenberg, D.; Muller, S. *J. Biol. Chem.* **2000**, *275*, 9043.
- Herceg, Z.; Wang, Z. Q. *Mol. Cell. Biol.* **1999**, *19*, 5124.
- Yu, S.-W.; Wang, H.; Poitras, M. F.; Coombs, C.; Bowers, W. J.; Federoff, H. J.; Poirer, G. G.; Dawson, T. M.; Dawson, V. L. *Science* **2002**, *297*, 259.
- Menissier-de Murcia, J.; Molinete, M.; Gradwohl, G.; Simonin, F.; de Murcia, G. *J. Mol. Biol.* **1989**, *210*, 229.
- Rolli, V.; O'Farrell, M.; Menissier-de Murcia, J.; de Murcia, G. *Biochemistry* **1997**, *36*, 12147.
- Jeggo, P. A. *Curr. Biol.* **1998**, *8*, R49.
- Griffin, R. J.; Pemberton, L. C.; Rhodes, D.; Bleasdale, C.; Bowman, K.; Calvert, A. H.; Curtin, N. J.; Durkacz, B. W.; Newell, D. R.; Porteous, J. K. *Anti-Cancer Drug Des.* **1995**, *10*, 507.

8. Nagayama, T.; Simon, R. P.; Chen, D.; Henshall, D. C.; Pei, W.; Stetler, R. A.; Chen, J. *J. Neurochem.* **2000**, *74*, 1636.
9. Takahashi, K.; Pieper, A. A.; Croul, S. E.; Zhang, J.; Snyder, S. H.; Greenberg, J. H. *Brain Res.* **1999**, *829*, 46.
10. Eliasson, M. J.; Sampei, K.; Mandir, A. S.; Hurn, P. D.; Traystman, R. J.; Bao, J.; Pieper, A.; Wang, Z. Q.; Dawson, T. M.; Snyder, S. H.; Dawson, V. L. *Nat. Med.* **1997**, *3*, 1089.
11. Pieper, A. A.; Walles, T.; Wei, G.; Clements, E. E.; Verma, A.; Snyder, S. H.; Zweier, J. L. *Mol. Med.* **2000**, *6*, 271.
12. Szabo, C.; Dawson, V. L. *Trends Pharmacol. Sci.* **1998**, *19*, 287.
13. Soriano, F. G.; Pacher, P.; Mabley, J.; Liaudet, L.; Szabo, C. *Circ. Res.* **2001**, *89*, 684.
14. Burkart, V.; Wang, Z. Q.; Radons, J.; Heller, B.; Herceg, Z.; Stingl, L.; Wagner, E. F.; Kolb, H. *Nat. Med.* **1999**, *5*, 314.
15. Akiyama, T.; Takasawa, S.; Nata, K.; Kobayashi, S.; Abe, M.; Shervani, N. J.; Ikeda, T.; Nakagawa, K.; Unno, M.; Matsuno, S.; Okamoto, H. *Proc. Natl. Acad. Sci. U.S.A.* **2001**, *98*, 48.
16. Watson, C. Y.; Whish, W. J. D.; Threadgill, M. D. *Bioorg. Med. Chem.* **1998**, *6*, 721.
17. Suto, M. J.; Turner, W. R.; Arundel-Suto, C. M.; Werbel, L. M.; Sebolt-Leopold, J. S. *Anti-Cancer Drug Des.* **1991**, *7*, 107.
18. Li, J. H.; Serdyuk, L.; Ferraris, D. V.; Xiao, G.; Tays, K.; Kletzly, P. W.; Li, W.; Lautar, S.; Zhang, J.; Kalish, V. *Bioorg. Med. Chem. Lett.* **2001**, *11*, 1687.
19. Abdelkarim, G. E.; Gertz, K.; Harms, C.; Katchanov, J.; Dirnagl, U.; Szabo, C.; Endres, M. *Int. J. Mol. Med.* **2001**, *7*, 255.
20. White, A. W.; Almassy, R.; Calvert, A. H.; Curtin, N. J.; Griffin, R. J.; Hostomsky, Z.; Maegley, K.; Newell, D. R.; Srinivasan, S.; Golding, B. T. *J. Med. Chem.* **2000**, *43*, 4084.
21. Banasik, M.; Komura, H.; Shimoyama, M.; Ueda, K. *J. Biol. Chem.* **1992**, *267*, 1569.
22. Li, H.; Goldstein, B. M. *J. Med. Chem.* **1992**, *35*, 3560.
23. Skalitzy, D. J.; Marakovits, J. T.; Maegley, K. A.; Ekker, A.; Yu, X.-H.; Hostomsky, Z.; Webber, S. E.; Eastman, B. W.; Almassy, R.; Li, J.; Curtin, N. J.; Newell, D. R.; Calvert, A. H.; Griffin, R. J.; Golding, B. T. *J. Med. Chem.* **2003**, *46*, 210.
24. Canan Koch, S. S.; Thoresen, L. H.; Jayashree, G. T.; Maegley, K. A.; Almassy, R. J.; Li, J.; Yu, X.-H.; Zook, S. E.; Kumpf, R. A.; Zhang, C.; Boritzki, T. J.; Mansour, R. N.; Zhang, K. E.; Ekker, A.; Calabrese, C. R.; Curtin, N. J.; Kyle, S.; Thomas, H. D.; Wang, L.-Z.; Calvert, A. H.; Golding, B. T.; Griffin, R. J.; Newell, D. R.; Webber, S. E.; Hostomsky, Z. *J. Med. Chem.* **2002**, *45*, 4961.
25. Kukla, M. J.; Breslin, H. J.; Pauwels, R.; Fedde, C. L.; Miranda, M.; Scott, M. K.; Sherrill, R. G.; Raeymaekers, A.; Van Gelder, J.; Andries, K.; Janssen, M. A.; De Clercq, E.; Janssen, P. A. J. *J. Med. Chem.* **1991**, *34*, 746.
26. Denny, W. A.; Rewcastle, G. W.; Baguley, B. C. *J. Med. Chem.* **1990**, *33*, 814.
27. McDonald, M. C.; Mota-Filipe, H.; Wright, J. A.; Abdelrahman, M.; Threadgill, M. D.; Thompson, A. S.; Thiemermann, C. *Br. J. Pharmacol.* **2000**, *130*, 843.
28. Geneste, P.; Kamenka, J.-M.; Vidal, Y.; Fauquet, J.-P.; Morel, M. E.; Muller, P.; Warolin, C. *Eur. J. Med. Chem.* **1978**, *13*, 53.
29. Ruf, A.; Rolli, V.; de Murcia, G.; Schulz, G. E. *J. Mol. Biol.* **1998**, *278*, 57.
30. Ruf, A.; de Murcia, G.; Schulz, G. E. *Biochemistry* **1998**, *37*, 3893.
31. Constantino, G.; Macchiarulo, A.; Camaioni, E.; Pelli-ciari, R. *J. Med. Chem.* **2001**, *44*, 3786.
32. Mandagere, A. K.; Thompson, T. N.; Hwang, K.-K. *J. Med. Chem.* **2002**, *45*, 304.
33. Arturrson, P. *J. Pharm. Sci.* **1990**, *79*, 476.
34. Belayev, L. *Stroke* **1996**, *27*, 1616.
35. Chen, S. T. *Stroke* **1986**, *17*, 738.
36. Breslin, H. J.; Kukla, M. J.; Ludovici, D. W.; Mohrbacher, R.; Ho, W.; Miranda, M.; Rodgers, J. D.; Hitchens, T. K.; Leo, G.; Gauthier, D. A.; Ho, C. Y.; Scott, M. K.; De Clercq, E.; Rauwels, R.; Andries, K.; Janssen, M. A.; Janssen, P. A. J. *J. Med. Chem.* **1995**, *38*, 771.
37. Ruf, A.; de Murcia, J. M.; de Murcia, G. M.; Schultz, G. E. *Proc. Natl. Acad. Sci. U.S.A.* **1996**, *93*, 7481.
38. Halgren, T. *J. Comp. Chem.* **1999**, *20*, 720.
39. Fleisher, D. *Peptide-based Drug Design: Controlling Transport and Metabolism*; American Chemical Society: Washington, DC, 1995.
40. Tokunaga, H.; Yoneda, Y.; Kuriyama, K. *Eur. J. Pharmacol.* **1983**, *87*, 237.
41. Takahashi, K.; Greenberg, J. H.; Jackson, P.; Maclin, K.; Zhang, J. *J. Cereb. Blood Flow Metab.* **1997**, *17*, 1137.